



# Milankovitch-scale environmental variation in the Banda Sea over the past 820 ka: Fluctuation of the Indonesian Throughflow intensity

Yin-Sheng Huang<sup>a,\*</sup>, Teh-Quei Lee<sup>b</sup>, Shu-Kun Hsu<sup>a</sup>

<sup>a</sup> Institute of Geophysics, National Central University, Chung-Li, Taiwan

<sup>b</sup> Institute of Earth Science, Academia Sinica, Taipei, Taiwan

## ARTICLE INFO

### Article history:

Available online 17 September 2010

### Keywords:

Banda Sea  
Milankovitch cycle  
Indonesian Throughflow  
Mid-Brunhes event

## ABSTRACT

We describe the environmental variation in the Banda Sea over the past 820 ka by using the magnetic parameters and oxygen isotope data from the core MD012380. Overall, characteristics of the magnetic parameters show simultaneous variation with marine isotope stage (MIS), especially in the last 420 ka. There are fewer, coarser and more oxidative magnetic minerals in glacial periods, and turn to opposite conditions in interglacial periods. Spectral results clearly present the Milankovitch periods over the last 820 ka, especially the eccentricity period (400-ka and 100-ka). However, the magnetic data shows different pattern before and after 420 ka. Thus, we segmented the time-series data into two periods: MIS 20 to MIS 12 and MIS 11 to MIS 1. During MIS 20 to MIS 12, the spectra of magnetic data show clear periods related to the obliquity (41-ka) and precession (23-ka and 19-ka), while they present only the eccentricity period (100-ka) during MIS 11 to MIS 1. This feature, which splits the late Pleistocene at around 420 ka, could be attributed to the mid-Brunhes event (MBE). In the Banda Sea, main factor controlling the variation of the magnetic minerals is considered as the fluctuation of the Indonesian Throughflow (ITF) intensity due to sea-level change. Thus, the magnetic data show clear 400-ka and 100-ka periods (main MIS cycle). Besides, the eccentricity signals are relatively dominant in the last ~420 ka, implying that the ITF might become more important after the MBE in the Banda Sea.

© 2010 Elsevier Ltd. All rights reserved.

## 1. Introduction

With increasing evidences, the tropical ocean now has been considered as a key role of modulating global climate change on orbital/suborbital time scales in the last decade (Cane and Clement, 1999; Scott et al., 2002; Visser et al., 2003; Wang et al., 2003). One of the important regions in the tropical Pacific, the Western Pacific Warm Pool (WPWP), is the area with constantly high sea surface temperature (SST) over 28 °C (Yan et al., 1992). Located in the WPWP, the Banda Sea is also characterized by high SST and high net precipitation, approximately 2000 mm/year (Gagan et al., 2004). Sea-water circulation in the Banda Sea is dominated by the Indonesian Throughflow (ITF), which connects the sea-waters of the Pacific Ocean and the Indian Ocean. Surface water current and precipitation variation are also influenced by a biannual monsoon system, which the Inter-Tropical Convergence Zone (ITCZ) is considered as the driving force behind the variability. In austral summer, the ITCZ situating near/over northern Australia (Hobbs et al., 1998) leads to the northwest (NW) monsoon and the sea-water flows from the Java Sea into the Banda Sea (Fig. 1). In austral winter, on the contrary, the ITCZ shifting northward (Hobbs et al.,

1998) drives the monsoon and sea-water current in an opposite direction.

In the last glacial period, sea-level at the adjoining Timor Sea was approximately 125 m lower than that of the present day (Yokoyama et al., 2001). Large portions of the Java Sea, Arafura Sea and Timor Sea were exposed above sea-level (Fig. 1). This reduction of sea-level would significantly modify the sea-water circulation because many passages among the islands were closed. Modeling results indicated that the ITF intensity reduced in the last glacial period (Kuhnt et al., 2004). Also, a study from the Timor Sea reported that the fluctuation of the ITF intensity was modulated by the sea-level change (Holbourn et al., 2005). In general, glacial-interglacial variation which influences sea-level change can be conveniently explained by the Milankovitch theory. The theory is proposed that the amount of the solar radiation reaching the earth surface could trigger an ice age or warm up the earth. There are three main factors of the theory: the eccentricity, obliquity and precession whose mean periods are centered at 400-ka, 100-ka, 41-ka and 23-ka or 19-ka respectively.

In this paper, we present new time-series magnetic data obtained from the core MD012380, including magnetic susceptibility ( $\chi$ ), saturated isothermal remanent magnetization (SIRM), ARM/ $\chi$  (ARM: anhysteretic remanent magnetization) and  $S$ -ratio (defined as  $IRM_{-0.3T}/IRM_{0.95T}$ ). To understand the magnetic characteristics

\* Corresponding author. Tel.: +886 3 4227151 65639; fax: +886 3 4222044.  
E-mail address: [yinson@gmail.com](mailto:yinson@gmail.com) (Y.-S. Huang).

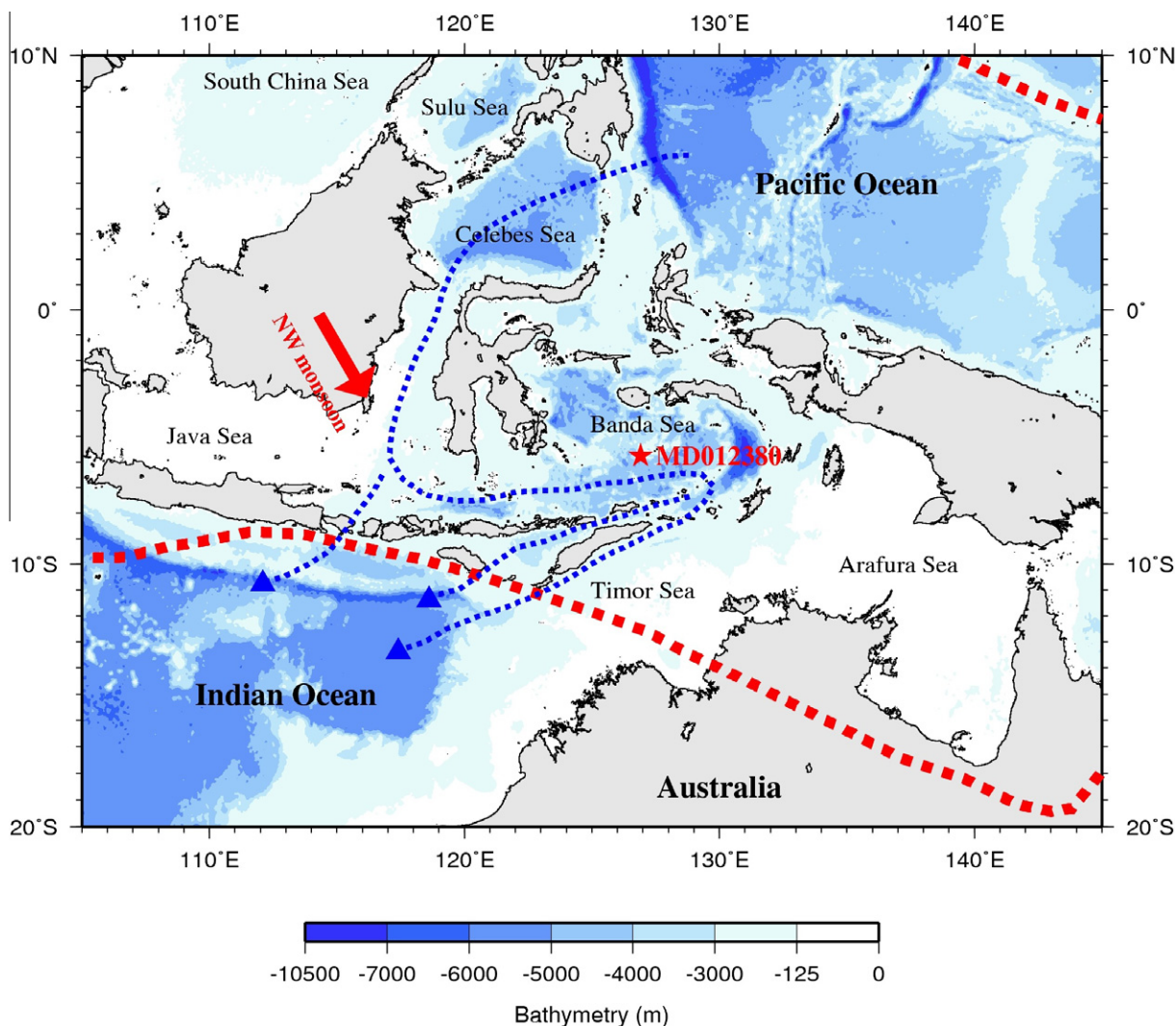


**Fig. 1.** Bathymetric map around the Banda Sea. Red star symbol is the location of the core MD012380. White areas indicate the regions where the water depth is shallower than 125 m. Blue dashed lines show the main paths of the Indonesian Throughflow. Red dashed lines are the position of the ITCZ in austral summer (southern hemisphere) and in austral winter (northern hemisphere). Red arrow represents the direction of the NW monsoon in austral summer. (For interpretation of the references to colour in this figure legend, the reader is referred to the web version of this article.)

in glacial/interglacial periods, we compare these records with the  $\delta^{18}\text{O}$  data from the same core (Chen et al., 2008). Furthermore, we compute the Fast Fourier Transform (FFT) spectrum to explain the periodicities related to the orbital forcing. Our purpose of the study is to understand the relationship among the magnetic data, their dominant periods and the environmental variation, especially the fluctuation of the ITF intensity, in the Banda Sea for the late Quaternary.

## 2. Material and methods

The core MD012380, with a total 39.9 m in length, was obtained from the Banda Sea (Lat.  $5^{\circ}45.64'S$ ; Long.  $126^{\circ}54.25'E$ ; water depth 3232 m; Fig. 1) during IMAGES (International Marine Global Change Study) VII Cruise in 2001. Core sediments are mostly composed of clay and silty clay with spotted pyrite, organic and glauconitic spots. Clay compositions are dominated by oozes with foraminifers and diatoms (Bassinot and Baltzer, 2001). There are only few bio-disturbances in the core so it provides good data for paleomagnetic analysis. All specimens were sampled by using a

U-channel with 1.5 m in length and then sequentially applied to the magnetic experiment.

The paleomagnetic experiments were performed in a magnetic shielding room to ensure that there was no external magnetic effect during measuring. All the measurements were sequentially measured with an interval of 1 cm. Magnetic susceptibility was measured by using the Bartington MS-2 magnetic susceptibility meter mounted on a long core system. Detailed alternating field (AF) demagnetization processes were done by using the 2G 755 SRM Superconducting Quantum Interference Device (SQUID) cryogenic magnetometer. The ARM was acquired by applying a 0.1 mT stable field within a 100 mT alternating field simultaneously, and then treated by AF demagnetization from 0 mT to 60 mT with 10 mT increment. Finally, a spiral-coil impulse magnetizer was used to induce the IRMs at peak field steps [25, 50, 75, 100, 150, 200, 250, 300, 500, 750 and 950 mT] progressively.

Based on the experiments, we obtained four magnetic parameters related to environmental variation, including magnetic susceptibility ( $\chi$ ), SIRM,  $\text{ARM}/\chi$  and  $S$ -ratio. Magnetic susceptibility generally measures the concentration of all magnetic minerals, while SIRM primarily relates to the change of the RM carriers, such

as magnetite and hematite (Opdyke and Channell, 1996). Both parameters give information about abundance of magnetic minerals of core sediments. Larger values of  $\chi$  and SIRM represent that there are more magnetic minerals, while smaller values indicate an opposite condition (Opdyke and Channell, 1996). S-ratio, defined as  $IRM_{-0.3T}/IRM_{0.95T}$  in the study, is associated with the change of magnetic mineralogy (Opdyke and Channell, 1996). S-ratio values close to one indicate the dominance of the ferrimagnetic mineralogy with lower coercivity, such as magnetite. The values decreasing away from one represent the increasing amount of higher coercivity magnetic minerals, such as hematite.  $ARM/\chi$  is conveniently used to identify relative grain size variation of magnetic minerals dominated by magnetite (King et al., 1982). Larger values of  $ARM/\chi$  indicate finer magnetic grains and lower values represent coarser magnetic grains in core sediments.

To reconstruct the age model of the core MD012380, four data sets were performed in the study, including the relative paleointensity (RPI) simulation,  $\delta^{18}O$  stratigraphy, accelerator mass spectrometry (AMS)  $^{14}C$  dating and biostratigraphy. The RPI simulation of the core was compared with the SINT-800 (Guyodo and Valet, 1999) to get the well controlled age points (Huang et al., 2009). Correlated with the low-latitude stack (Bassinot et al., 1994), the marine isotope stage (MIS) of the core was calibrated (Chen et al., 2008). The AMS  $^{14}C$  dating was applied on the upmost part of the core and analyzed by the Rafter Radiocarbon Laboratory, New Zealand. Last appearance datum (LAD) of the *Pseudoemiliana lacunosa*, delimited between 22.75 m and 31.81 m (about at 28.4 m), was provided an additional age control point at 458 ka (Berggren et al., 1995). In total, twenty-two age control points were used to establish the age model in the study (Fig. 2 and Table 1). The model shows that core MD012380 covers an age over the past  $\sim 820$  ka with a total depth of 39.9 m, implying an average sedimentation rate of  $\sim 4.8$  cm/ka.

For analyzing the periodicities recorded in the parameters, the FFT spectrum was applied. Because there are many regional and irregular signals in our paleomagnetic data, such as sharp peaks or troughs, we estimate the FFT power spectrum density (PSD) by applying the Welch-Overlapped-Segment-Averaging (WOSA)

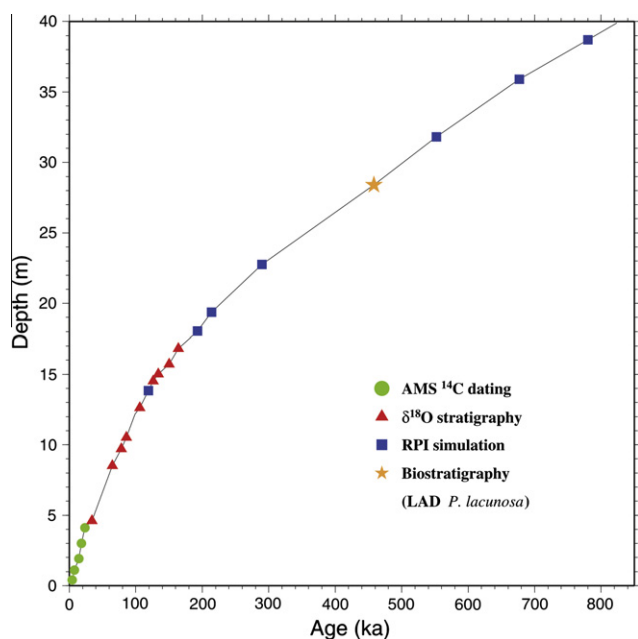


Fig. 2. Age model of the core MD012380. Four methods were applied to control the core age in the study, including the AMS  $^{14}C$  dating,  $\delta^{18}O$  stratigraphy, RPI simulation and biostratigraphy.

Table 1  
Age model of the core MD012380.

Depth (m)	Age (ka)	Method	
0.41	4.17	AMS $^{14}C$ dating	
1.11	7.71		
1.91	14.55		
3.01	18.34		
4.11	23.63		
4.61	34		
8.51	65		$\delta^{18}O$ stratigraphy (correlated to the low-latitude stack)
9.71	78		
10.51	86		
12.61	106		
14.51	126		
15.01	134		
15.71	150		
16.81	164		
13.84	119	RPI simulation (correlated to the SINT-800)	
18.05	193		
19.37	214		
22.75	290		
31.81	552	Biostratigraphy (LAD <i>P. lacunosa</i> )	
35.89	677		
38.70	780		
28.40	458		

method (Welch, 1967) in the study. Time-series data were segmented into three equal segments with 50% overlap by applying the Hanning window, and the obtained periodogram was averaged by the PSD of each segment. By using the WOSA method, the noises could be mostly average out and the signals become clearer.

### 3. Results

#### 3.1. Properties of the magnetic data

By applying the age model (Fig. 2 and Table 1), four time-series magnetic data could be obtained (Fig. 3). We compared these magnetic data with the  $\delta^{18}O$  (MIS) variation to study the magnetic characteristics in glacial/interglacial periods. Overall, four magnetic data show similar variation related to MIS change, especially in the last  $\sim 420$  ka: lower values in glacial periods and higher values in interglacial periods (Fig. 3). It indicates that the magnetic minerals are fewer, coarser and more oxidative in glacial periods, and turn to opposite conditions in interglacial periods.

A long-term trend is also observed in these magnetic records (Fig. 3b–e). The values of magnetic data decrease gradually from  $\sim 700$  ka to  $\sim 420$  ka and present a minimum at  $\sim 350$  ka, and then increase slowly after  $\sim 350$  ka. Besides, the magnetic parameters vary rapidly and frequently before  $\sim 420$  ka but show regular variation related to MIS change after  $\sim 420$  ka (Fig. 3b–e). Moreover, there are several clear peaks appeared in both  $\chi$  and SIRM before 420 ka, especially between 700 ka and 600 ka (Fig. 3b–c). The most notable event recorded in all data is observed between  $\sim 80$  ka and  $\sim 40$  ka (Fig. 3b–e). This event indicates that magnetic minerals suddenly became fewer, coarser and more oxidative in MIS 4 though the feature is ambiguous in the  $\delta^{18}O$  data (Fig. 3a). These features may be caused by environmental events and we will discuss the details in the later section.

#### 3.2. Orbital signals

It is generally accepted that main cycle of MIS variation is 100-ka period (Broecker and van Donk, 1970), which could be related to the glacial-interglacial variation. Chen et al. (2008) reported that the  $\delta^{18}O$  spectrum of the core MD012380 shows the 100-ka period. In our study, the values of magnetic data also show variation

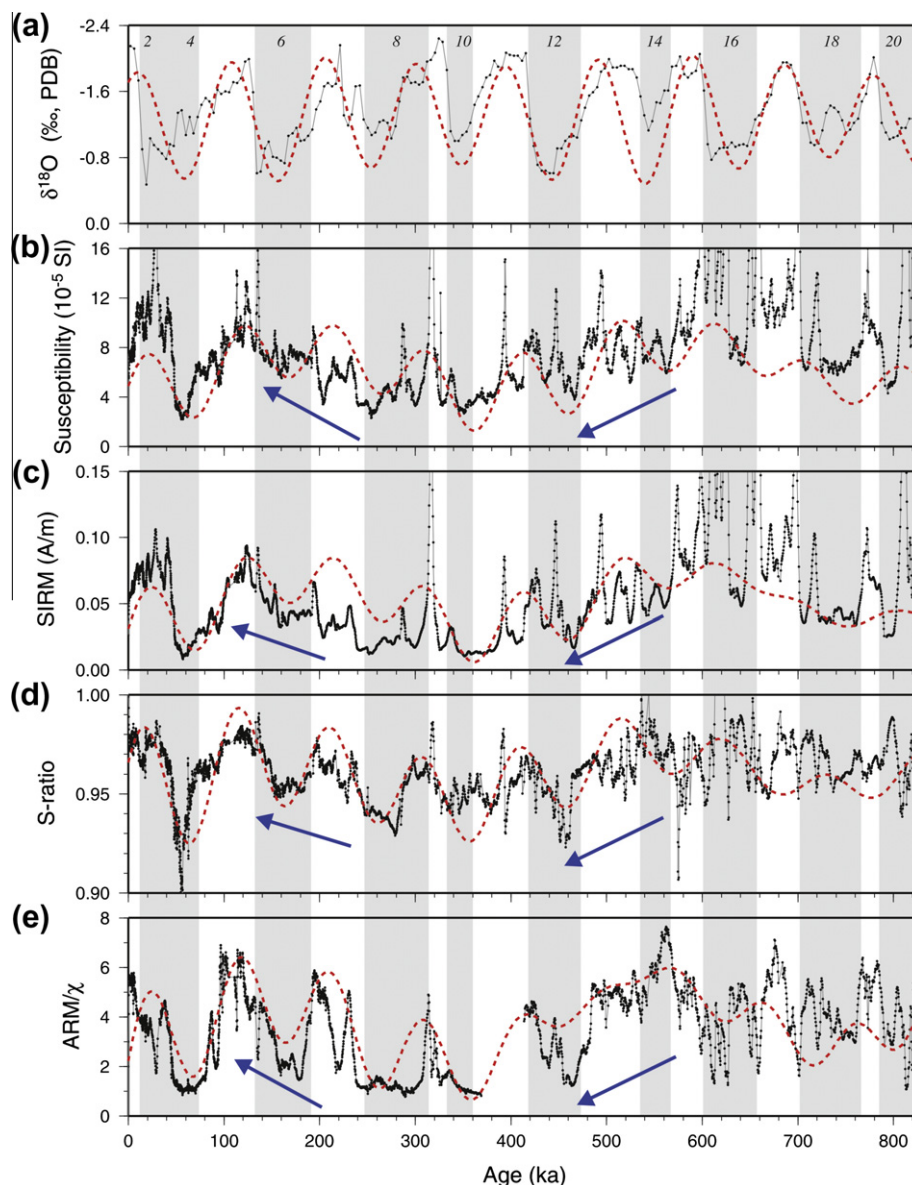


**Fig. 3.** Time-series data including (a)  $\delta^{18}\text{O}$  record, (b) magnetic susceptibility, (c) SIRM, (d)  $S$ -ratio and (e)  $\text{ARM}/\chi$ . Gray/white areas indicate the identified glacial/interglacial periods and the numbers give the glacial stages respectively. Red dashed lines show the eccentricity signal for each parameter. Blue arrows mark the long-term trend recorded in the magnetic data. (For interpretation of the references to colour in this figure legend, the reader is referred to the web version of this article.)

related to the main MIS change and present a long-term trend. To understand more about these magnetic characteristics, we furthermore extracted the eccentricity signal, which is composed of 100-ka and 400-ka periods, for each parameter (red dashed lines in Fig. 3).

Unquestionably, good relationship is shown between the eccentricity signal and the  $\delta^{18}\text{O}$  data (Fig. 3a). Amplitudes of both signals are about the same and become weaker before  $\sim 600$  ka. As for the magnetic parameters, all of them present similar patterns. Better relationship between the eccentricity signals and magnetic records is observed after  $\sim 420$  ka, especially in the last  $\sim 200$  ka (Fig. 3b–e). However, the relationship is ambiguous and the amplitude becomes weaker in the older ages. The long-term trend embedded in the magnetic data could also be evidently related to the long eccentricity period (400-ka) and present a minimum at  $\sim 350$  ka (Fig. 3b–e). Besides, it seems that the eccentricity signals of the magnetic data are in advance of the  $\delta^{18}\text{O}$  data (Fig. 3), although it is difficult to quantify the value.

### 3.3. FFT power spectra

For further study, power spectral analyses based on the WOSA FFT method were applied to all the data. The  $\delta^{18}\text{O}$  record is firstly analyzed and its spectrum clearly shows the Milankovitch periods centered at 400-ka, 100-ka, 41-ka and 23-ka in addition to a non-orbital 30-ka period (Fig. 4).

As for the magnetic records, both  $\chi$  and SIRM spectra show similar periodicities centered at 400-ka, 100-ka, 60-ka,  $\sim 41$ -ka (45-ka and 43-ka), 34-ka, 26-ka, 22-ka, 20-ka and 18-ka (Fig. 5a and b). The  $S$ -ratio spectrum presents four minor periods centered at 41-ka, 30-ka, 25-ka and 19-ka besides three dominant periods, 400-ka, 100-ka and 60-ka (Fig. 5c). Unlike the other magnetic records, the  $\text{ARM}/\chi$  spectrum shows similar periodicities to the  $\delta^{18}\text{O}$  spectrum. The dominant periods center at 400-ka, 100-ka, 41-ka, 30-ka and 21-ka (Fig. 5d). These observed periodicities could be easily attributed to the orbital forcing including the eccentricity (400-ka and 100-ka), obliquity (45-ka and 43-ka) and precession

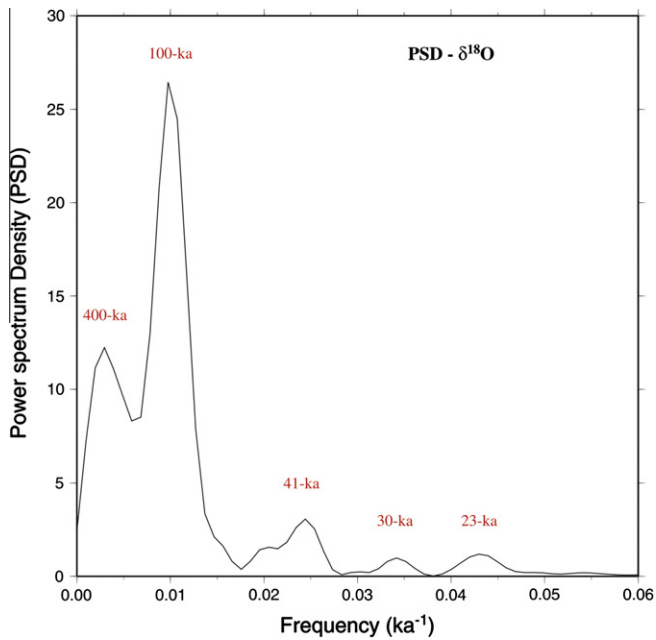


Fig. 4. Spectrum result of the  $\delta^{18}\text{O}$  data of the core MD012380. The Milankovitch periods are clearly presented besides a 30-ka period.

(26-ka, 25-ka, 22-ka, 21-ka, 20-ka, 19-ka and 18-ka). However, two non-orbital periods centered at 60-ka and 30-ka are also presented in the spectra.

#### 4. Discussion

##### 4.1. Magnetic characteristic in glacial/interglacial periods

Based on the results, we have understood that magnetic minerals vary with MIS change simultaneously, especially in the last  $\sim 420$  ka (Fig. 3). Chen et al. (2008) proposed that the planktonic foraminiferal  $\delta^{18}\text{O}$  record of the Banda Sea is influenced by the SST change, ice-volume effect and local salinity variation. For inorganic magnetic minerals, we suggest that fluctuations of magnetic minerals might be mostly controlled by the ocean circulation related to ice-volume effect (sea-level change). At present, the ITF is considered as an important factor controlling the ocean current in the Banda Sea. However, in glacial periods, many passages of the ITF would close because of sea-level reduction. A model describing the Neogene history of the ITF indicated a decrement of the ITF intensity in the last glacial period (Kuhnt et al., 2004). A study from the Timor Sea had also suggested that the ITF intensity was modulated by sea-level change (Holbourn et al., 2005).

In our study, variation of the magnetic characteristics is in agreement with the past studies. In glacial periods, the ITF inten-

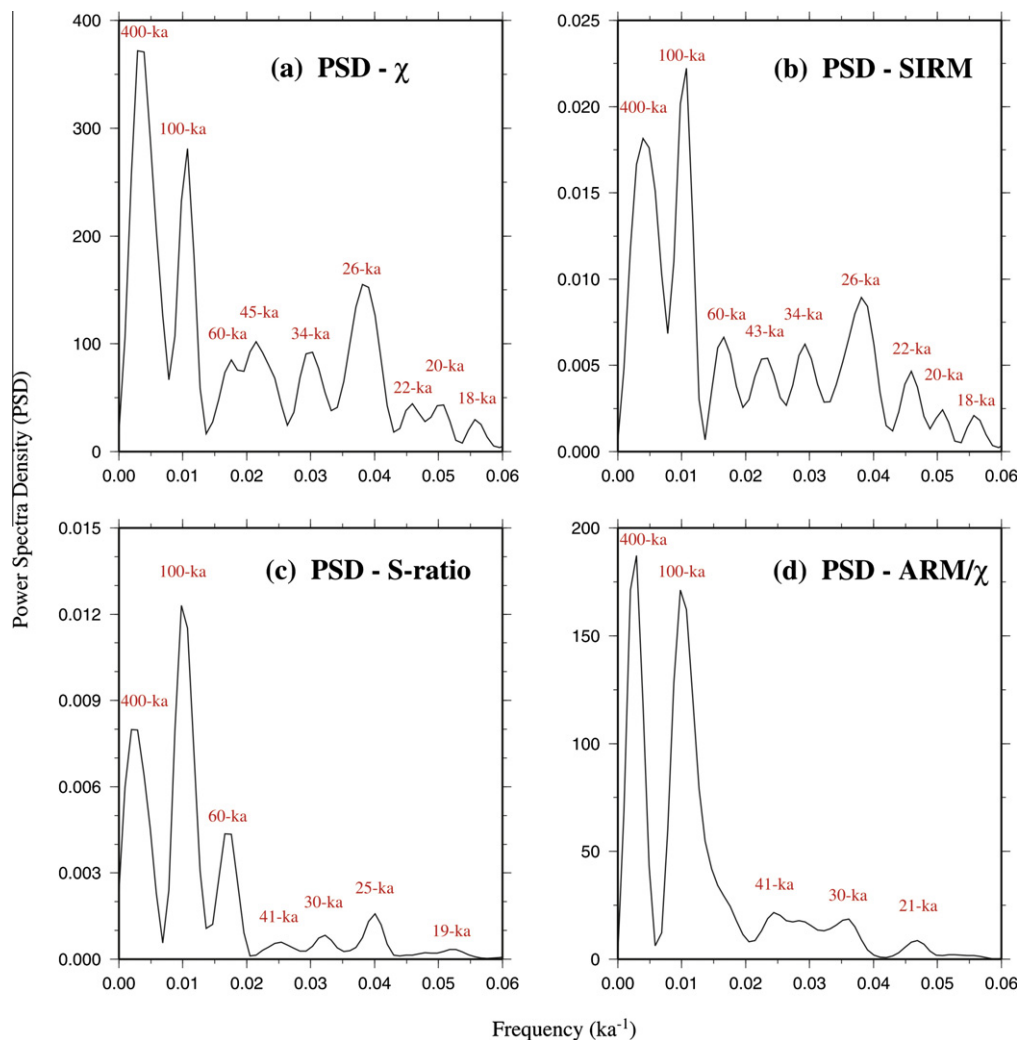


Fig. 5. Spectral results of the magnetic records of the core MD012380, including (a) magnetic susceptibility, (b) SIRM, (c) S-ratio and (d)  $\text{ARM}/\chi$ .

sity decreased so the magnetic minerals brought by the ITF would become fewer and coarser. Besides, more land exposed above sea-water due to the reduction of sea-level. Coarser and more oxidative minerals from the land would be brought into the sea because of stronger weathering and erosion. On the contrary, there should be more, finer and less oxidative magnetic minerals due to the opposite environmental conditions in interglacial periods.

The long-term trend, observed in the magnetic records (Fig. 3), might also be related to the fluctuation of the ITF intensity caused by sea-level change. It implies that both 400-ka and 100-ka eccentricity cycles may dominate the ITF intensity in the Banda Sea. Moreover, a notable event is observed between  $\sim 80$  ka and  $\sim 40$  ka in the magnetic records though there is no similar feature found in  $\delta^{18}\text{O}$  data (Fig. 3). We considered that there was a larger

reduction of sea-level in MIS 4 but more evidences are needed for further explanation.

#### 4.2. Milankovitch cycles

We had extracted the eccentricity signal for each record and found it could evidently describe the main variation of each record (Fig. 3). We furthermore extracted the ETP signal (composed of 400-ka, 100-ka, 41-ka, 23-ka and 19-ka) for each record respectively (Fig. 6) because all the spectra present the clear Milankovitch periods (Figs. 4 and 5). Overall, the ETP signals of all the magnetic data vary simultaneously with that of the  $\delta^{18}\text{O}$  data after  $\sim 420$  ka (Fig. 6). However, the signals are relatively complex and inconsistent, and the amplitudes are weaker before  $\sim 420$  ka. This feature is

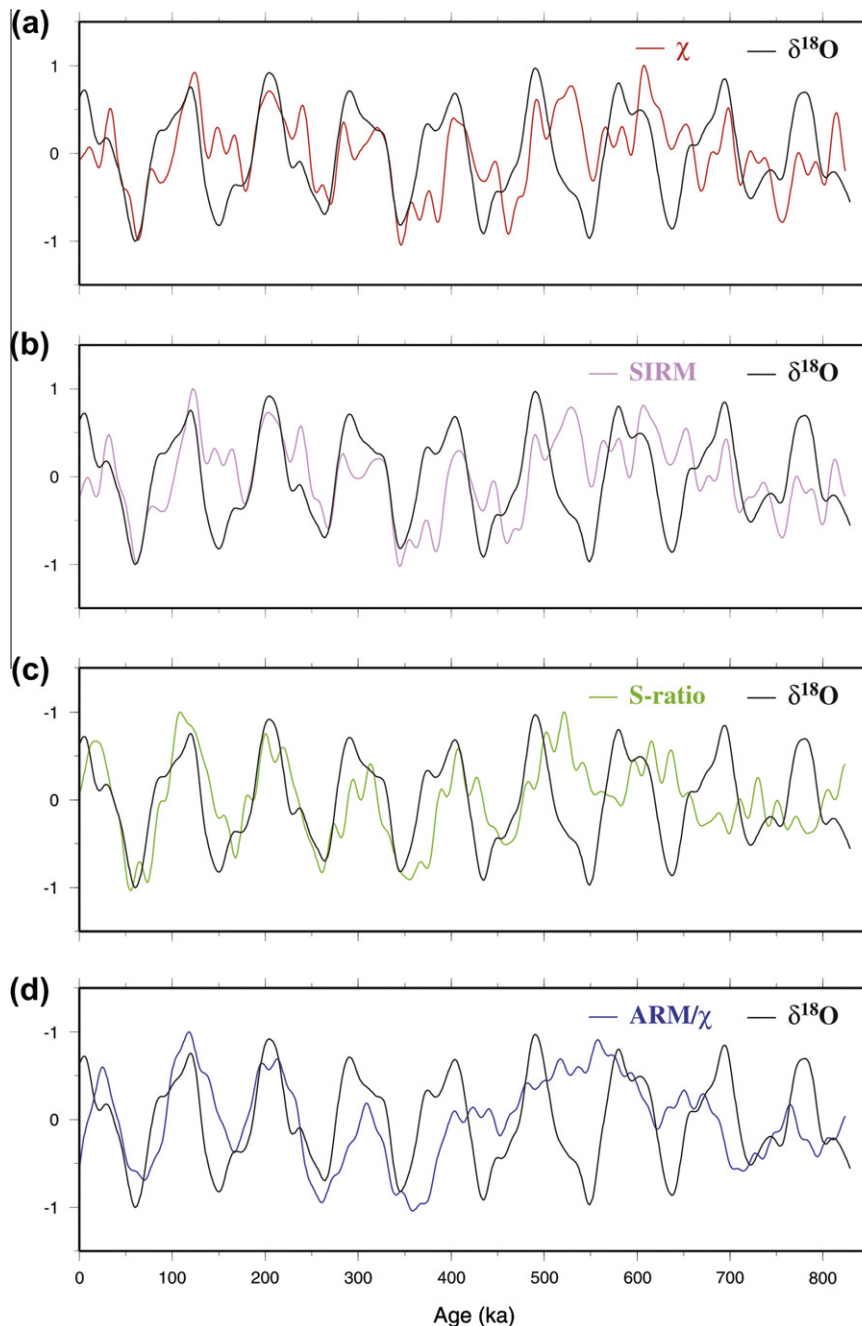


**Fig. 6.** The comparison of the ETP signals (composed of 400-ka, 100-ka, 41-ka, 23-ka and 19-ka periods) between the  $\delta^{18}\text{O}$  data and the magnetic records, including (a) magnetic susceptibility, (b) SIRM, (c) S-ratio and (d)  $\text{ARM}/\chi$ .

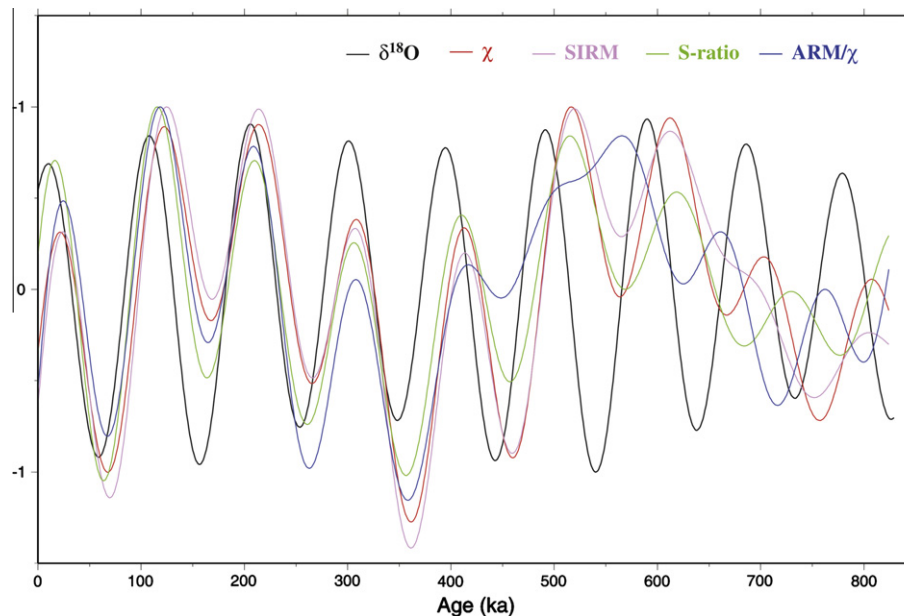


Fig. 7. The eccentricity signals (composed of 400-ka and 100-ka periods) of the used data of the core MD012380. The signals are complex before 420 ka and become regular in the last 420 ka.

more distinct if we arrange only the eccentricity signals together (Fig. 7). It implies that the factors controlling the environmental variation are relative simplification in the last  $\sim 420$  ka. Besides, the ETP signals of the magnetic data are likely in advance of that of the  $\delta^{18}\text{O}$  record, but it is difficult to quantify the value. We may roughly estimate the value of this phase difference by using the eccentricity signals instead. The eccentricity signals of the magnetic records lead that of the  $\delta^{18}\text{O}$  data about  $18^\circ$  to  $36^\circ$  in the last  $\sim 420$  ka. The reason of this phase difference might be suggested: The detrital magnetic minerals would vary instantly with the fluctuation of the ITF intensity, while the  $\delta^{18}\text{O}$  data might deposit secondly due to some organic processes.

Except for the typical Milankovitch periods, we find some quasi-obliquity periods (45-ka and 43-ka) and quasi-precession periods (26-ka, 25-ka, 22-ka, 21-ka, 20-ka, and 18-ka) in the spectra of magnetic data (Fig. 5). These periods close to the obliquity and precession cycles could also be attributed to the orbital forcing though they present a little bias somehow. Moreover, a 60-ka period is appeared except for the ARM/ $\chi$  spectrum, and a  $\sim 30$ -ka period is found in all spectra (Fig. 5). Muller and MacDonald (2000) reported that the obliquity consisted of a clear 41-ka period with two weak periods centered at 53-ka and 29-ka. Therefore, the 60-ka and 30-ka periods may also be explained as the obliquity signals.

Besides, Pisias and Rea (1988) reported that the 30-ka period is commonly recorded in climatic proxies, especially in the Pacific Ocean. A different aspect about the 30-ka period was proposed as reflecting the variation of the El Niño-Southern Oscillation (ENSO) variability (Beaufort et al., 2001). Such ENSO-like period (30-ka) is also recorded in the marine sediment core from the adjoining Timor Sea (Kershaw et al., 2003).

#### 4.3. Mid-Brunhes event

From the line discussing above, we have known that different variation pattern is presented before and after  $\sim 420$  ka, especially in the magnetic records. The feature implies that there might be an environmental event at around 420 ka. Therefore, we segmented the time-series data into two periods at 420 ka, that is, MIS 20 to MIS 12 and MIS 11 to MIS 1. During MIS 20 to MIS 12, the  $\delta^{18}\text{O}$

spectrum shows only a clear period close to 100-ka (Fig. 8). However, the spectra of  $\chi$  and SIRM present obvious PSD signals centered at the periods of obliquity (40-ka) and precession (22-ka, 20-ka and 19-ka) besides the 100-ka period. The S-ratio spectrum shows a clear period centered at about 70-ka, and two minor periods (125-ka and 23-ka) are also appeared. Similar to the spectra of  $\chi$  and SIRM, the ARM/ $\chi$  spectrum presents clear periods centered at 100-ka and 40-ka though there is ambiguous period related to the precession. On the contrary, the spectra of all data present an obvious 100-ka period during MIS 11 to MIS 1.

This dramatic feature, which splits the late Pleistocene at around 420 ka, could be attributed to the mid-Brunhes event (MBE). The MBE is characterized by showing an asymmetric climate conditions between the Northern Hemisphere (NH) and Southern Hemispheres (SH) around the middle Brunhes epoch (Jansen et al., 1986). Climate was colder (glacial conditions) in the NH while it became warmer (interglacial conditions) in the SH and equatorial regions. Because of the warmer climate conditions, sea-level might be higher in equatorial regions. It confirms our suggestion that sea-level might rise gradually in the last  $\sim 420$  ka. Because of sea-level raise, the ITF intensity might increase and become dominant in the Banda Sea. The magnetic minerals dominated by the ITF therefore become relative simplification with a main period centered at 100-ka in the last 420 ka.

## 5. Conclusion

Over the past 820 ka, the magnetic minerals show simultaneous variation with MIS change in the Banda Sea. This variation could be attributed to the fluctuation of the ITF intensity. In glacial periods, the ITF intensity might decrease because of sea-level reduction. The magnetic minerals brought by the ITF therefore become fewer, coarser and more oxidative. On the contrary, there should be more, finer and less oxidative magnetic minerals due to the opposite environmental conditions in interglacial periods. As for the FFT spectral results, all spectra clearly show the Milankovitch periods in the study, especially the 400-ka and 100-ka periods (main MIS cycle). It also implies that the fluctuation of the ITF intensity might be dominated by sea-level change. Moreover, the dominant orbital

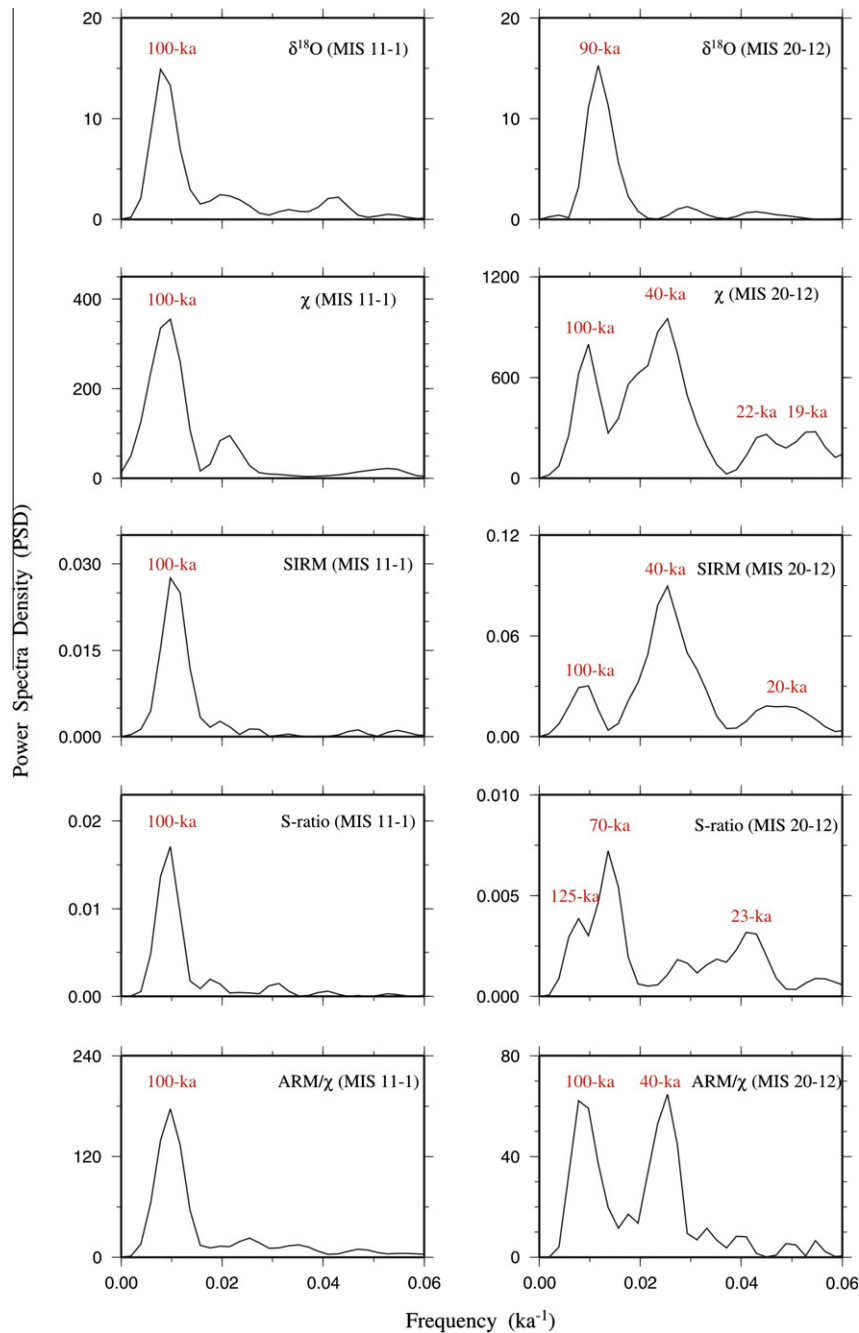


**Fig. 8.** Segmented spectra of the used data in the study. The time-series data is segmented into two periods at 420 ka, that is, MIS 20 to MIS 12 and MIS 11 to MIS 1. Different orbital periods are present in two periods clearly.

periods, recorded in the magnetic data, are entirely different before and after  $\sim 420$  ka. Values of the magnetic data vary rapidly, and show periods related to the obliquity and precession before  $\sim 420$  ka. But they become relative simplification and present only a clear 100-ka period in the last  $\sim 420$  ka. The feature splitting the late Pleistocene at around 420 ka could be attributed to the MBE. From the results of the segmented spectra, we could also suggest that the ITF is more dominant in the Banda Sea after the MBE.

#### Acknowledgements

We would like to express our appreciation to all the researchers and staffs on the *R.V. Marion Dufresne*, during the IMAGES Cruise VII, to collect such a high quality core from the Banda Sea. Also

we like to acknowledge the National Core Laboratory located at the National Taiwan Ocean University for the help of sampling the core; members in the Paleomagnetic Laboratory, institute of Earth Sciences, Academia Sinica for helping on the magnetic experiments and members of the Marine Geophysical Research group, National Central University for valuable discussion. The Financial support came from the National Science Council of Taiwan under the Grant NSC91-2611-M-001-003-IM. The figures were plotted by using the GMT software (Wessel and Smith, 1998).

#### References

- Bassinot, F.C., Labeyrie, L.D., Vincent, E., Quidelleur, X., Shackleton, N.J., Lancelot, Y., 1994. The astronomical of climate and the age of the Brunhes-Matuyama magnetic reversal. *Earth Planet. Sci. Lett.* 123, 91–108.

- Bassinot, F., Baltzer, A., 2001. On Board Report of WEPAMA Cruise MD122/ IMAGES VII. RV Marion Dufresne, p. 133.
- Beaufort, L., de Garidel-Thoron, T., Mix, A.C., Pisias, N.G., 2001. ENSO-like forcing on oceanic primary production during the Late Pleistocene. *Science* 293, 2440–2444.
- Berggren, W.A. et al., 1995. Late neogene chronology: new perspectives in high-resolution stratigraphy. *GSA Bull.* 107 (11), 1272–1287.
- Broecker, W.S., van Donk, J., 1970. Insolation changes, ice volumes, and the  $\delta^{18}\text{O}$  record in deep-sea cores. *Rev. Geophys. Space Phys.* 8, 169–197.
- Cane, M., Clement, A., 1999. A role for the tropical Pacific coupled ocean-atmosphere system on Milankovitch and millennial time-scales, part II: Global impacts. In: Clark, P.U., Webb, R.S., Keigwin, L.D., (Eds.), *Mechanisms of Global Climate Change at Millennial Scales*, vol. 112. *Geophys. Monogr. Ser.*, AGU, Washington, DC, pp. 373–393.
- Chen, C.W., Wei, K.Y., Mii, H.S., Yang, T.N., 2008. A late quaternary planktonic foraminiferal oxygen isotope record of the Banda Sea: chronostratigraphy, orbital forcing, and paleoceanographic implications. *Terr. Atmos. Ocean. Sci.* 19, 331–339.
- Gagan, M.K., Hendy, E.J., Haberle, S.G., Hantoro, W.S., 2004. Post-glacial evolution of the Indo-Pacific warm pool and El Nino-Southern Oscillation. *Quatern. Int.* 118, 127–143.
- Guyodo, Y., Valet, J.P., 1999. Global changes in intensity of the Earth's magnetic field during the past 800 kyr. *Nature* 399, 249–252.
- Hobbs, J.E., Lindesay, J.A., Bridgman, H.A., 1998. *Climates of the Southern Continents: Present, Past and Future*. John Wiley & Sons, Ltd., West Sussex, England. pp. 63–100.
- Holbourn, A., Kuhnt, W., Kawamura, H., Jian, Z., Grootes, P., Erlenkeuser, H., Xu, J., 2005. Orbitally paced paleoproductivity variation in the Timor Sea and Indonesian throughflow variability during the last 460 kyr. *Paleoceanography* 20 (PA3002), 1–18.
- Huang, Y.S., Lee, T.Q., Hsu, S.K., Yang, T.N., 2009. Paleomagnetic field variation with strong negative inclination during the Brunhes chron at the Banda Sea, equatorial southwestern Pacific. *Phys. Earth Planet. Int.* 173, 162–170.
- Jansen, J.H.F., Kuijpers, A., Troelstra, S.R., 1986. A mid-Brunhes climatic event: long-term changes in global atmosphere and ocean circulation. *Science* 232, 619–622.
- Kershaw, A.P., van der Kaars, S., Moss, P.T., 2003. Late Quaternary Milankovitch-scale climatic change and variability and its impact on monsoonal Australasia. *Mar. Geol.* 201, 81–95.
- King, J.W., Banerjee, S.K., Marvin, J., Ozdemir, O., 1982. A comparison of different magnetic methods for determining the relative grain size of magnetite in nature materials: some results from lake sediments. *Earth Planet. Sci. Lett.* 59, 404–419.
- Kuhnt, W., Holbourn, A., Hall, R., Zuvella, M., Käse, R., 2004. Neogene history of the Indonesian throughflow. In: Clift, P., Wang, P., Kuhnt, W., Hayes, D.E. (Eds.), *Continent–Ocean Interactions within the East Asian Marginal Seas*, vol. 149. *AGU Geophysical Monograph*. pp. 299–320.
- Muller, R.A., MacDonald, G.J., 2000. *Ice Ages and Astronomical Causes: Data, Spectral Analysis and Mechanisms*. Springer-PRAXIS, Chichester, UK. pp. 1–318.
- Opdyke, N.D., Channell, J.E.T., 1996. Magnetic parameters sensitive to concentration, grain size and mineralogy. In: *Magnetic Stratigraphy*. Academic Press, USA, pp. 251–253.
- Pisias, N.G., Rea, D.K., 1988. Late Pleistocene paleoclimatology of the central equatorial Pacific: sea surface response to the southeast trade winds. *Paleoceanography* 3, 21–37.
- Scott, L., Poulsen, C., Lund, S., Thunell, R., 2002. Super ENSO and global climate oscillations at millennial time scales. *Science* 297, 222–226.
- Visser, K., Thunell, R., Scott, L., 2003. Magnitude and timing of temperature change in the Indo-Pacific warm pool during deglaciation. *Nature* 421, 152–155.
- Wang, P., Tian, J., Cheng, X., Liu, C., Xu, J., 2003. Carbon reservoir changes preceded major ice-sheet expansion at mid-Brunhes event. *Geology* 31, 239–242.
- Welch, P.D., 1967. The use of fast fourier transform for the estimation of power spectra: a method based on time averaging over short, modified periodograms. *IEEE Trans. Audio Electroacoustics* AU-15, 70–73.
- Wessel, P., Smith, W.H.F., 1998. New improved version of generic mapping tools released. *EOS Transaction AGU* 79, 579.
- Yan, X.H., Ho, C.R., Zheng, Q., Klemas, V., 1992. Temperature and size variabilities of the western Pacific warm pool. *Science* 258, 1643–1645.
- Yokoyama, Y., De Dekker, P., Lambeck, K., Johnston, P., Fifield, L.K., 2001. Sea-level at the last glacial maximum: evidence from northwestern Australia to constrain ice volumes for oxygen isotope stage 2. *Palaeogeography, Palaeoclimatology, Palaeoecology* 165, 281–297.